

## PAPER

[View Article Online](#)  
[View Journal](#) | [View Issue](#)Cite this: *Catal. Sci. Technol.*, 2025, 15, 1272

## Tungsten-dioxo single-site heterogeneous catalyst on carbon: synthesis, structure, and catalysis†

Amol Agarwal,<sup>a</sup> Yiqi Liu,<sup>b</sup> Miyuki Hanazawa,<sup>c</sup> Jiaqi Li,<sup>b</sup> Takayuki Nakamuro,<sup>c</sup> Eiichi Nakamura,<sup>c</sup> Yosi Kratish<sup>\*b</sup> and Tobin J. Marks<sup>\*b</sup>

This study investigates the application of a novel third-row metal, tungsten, to carbon-supported single-site metal-oxo heterogeneous catalysis. Tungsten is a green and earth-abundant metal, but an unexplored candidate in this role. The carbon (AC = activated carbon)-supported tungsten dioxo complex, AC/WO<sub>2</sub> was prepared via grafting of (DME)WO<sub>2</sub>Cl<sub>2</sub> (DME = 1,2-dimethoxyethane) onto high-surface-area activated carbon. AC/WO<sub>2</sub> was fully characterized by ICP-OES, XPS, EXAFS, XANES, SMART-EM, and DFT. W 4d<sub>7/2</sub> XPS and W L<sub>III</sub>-Edge XANES assign the oxidation state as W(VI), while EXAFS reveals two W=O double and two W–O single bonds at distances of 1.73 and 1.92 Å, respectively. These data align well with DFT computational results, supporting the structure as Carbon(–μ–O–)<sub>2</sub>M(=O)<sub>2</sub>. SMART-EM verifies that single W(VI) catalytic sites are bonded in an out-of-plane manner. The catalytic performance of air- and water-stable AC/WO<sub>2</sub> is compared to that of AC/MoO<sub>2</sub>. AC/WO<sub>2</sub> is more active and selective than the molybdenum analog in mediating alcohol dehydration of various substrates, and is recyclable. Notably, AC/WO<sub>2</sub> is an effective and recyclable catalyst for primary aliphatic alcohol dehydration and forms no dehydrogenation side products in contrast to AC/MoO<sub>2</sub>. However, AC/WO<sub>2</sub> is less effective in epoxidation and PET depolymerization. Overall, this work demonstrates the potential of carbon-supported third row metals for future studies.

Received 18th December 2024,  
Accepted 5th January 2025

DOI: 10.1039/d4cy01517g

[rsc.li/catalysis](https://rsc.li/catalysis)

## Introduction

Catalysts serve a vital function in diverse industries, ranging from energy production to healthcare to environmental management. Their application spans over 80% of industrial processes, highlighting their significance in driving reactions that generate more than one-third of the global economic output. By enhancing reaction rates and selectivity, catalysts not only improve productivity but also contribute to the development of sustainable technologies, making them indispensable in addressing modern chemical challenges.<sup>1,2</sup> Homogeneous and metalloenzymatic catalysis are typically well-characterized in terms of active site structures and

mechanisms, but their possible air-sensitivity, shorter lifespans, thermal instability, and catalyst-product separation challenges limit their industrial use. In contrast, heterogeneous catalysts are preferred for their durability and recyclability, although their complex structures and diverse surface sites complicate understanding-based new catalyst design. Therefore, a key goal in heterogeneous catalysis must be the knowledge-based design and creation of well-defined active sites that enhance atom economy, selectivity, and simplify mechanistic interpretation.

Single-site heterogeneous catalysts (SSHCs) provide a promising strategy to bridge homogeneous and heterogeneous catalysis by utilizing precisely defined molecular precursors. This approach yields isolated metal centers that are uniformly distributed and possess known coordination environments, increasing our understanding of their behavior.<sup>3–8</sup> Furthermore, the ability to finely tune these metal sites via ligand modifications is a significant attraction. In addition to conventional supports such as silica, alumina, other oxides, and carbon, known for their complex surface structures yet cost-effectiveness, there is a growing interest in developing better-defined supports as model catalysts to enable mechanistic studies such as using well-defined graphenes,<sup>9</sup> and carbon nanohorn (CNHs)<sup>10</sup> to better understand the role of the carbon supports.

<sup>a</sup> Department of Materials Science and Engineering, Trienens Institute for Sustainability and Energy, Northwestern University, 2145 Sheridan Road, Evanston, Illinois 60208, USA

<sup>b</sup> Department of Chemistry, Trienens Institute for Sustainability and Energy, Northwestern University, 2145 Sheridan Road, Evanston, Illinois 60208, USA. E-mail: yosi.kratish@northwestern.edu, t-marks@northwestern.edu

<sup>c</sup> Department of Chemistry, The University of Tokyo, 7-3-1 Hongo, Bunkyo-ku, Tokyo 113-0033, Japan. E-mail: muro@chem.s.u-tokyo.ac.jp, nakamura@chem.s.u-tokyo.ac.jp

† Electronic supplementary information (ESI) available. See DOI: <https://doi.org/10.1039/d4cy01517g>



Molybdenum, known for its versatile chemical reactivity, low toxicity, and natural abundance, plays a crucial role in the catalysis of many transformations.<sup>11,12</sup> Mo-oxo-based complexes are particularly important in metalloenzyme systems,<sup>13</sup> as well as in laboratory-scale and industrial catalytic processes.<sup>14</sup> Mo-oxo catalysts have also gained recognition for key organic transformations such as transesterification, hydrosilylation, olefin metathesis, hydroboration, and epoxidation.<sup>15–23</sup> While many of these reactions are reasonably well-understood mechanistically for homogenous Mo(vi) complexes owing to their well-defined molecular-level structures, the active sites of their heterogenous counterparts remain less well-defined. Thus, the possibility of rationally designing Mo-based SSHC systems in which the surface catalytic sites and their reactivity reasonably are well-defined presents intriguing possibilities.

Previously we reported the first Mo-oxo SSHCs supported on activated carbon, AC/MoO<sub>2</sub> (Fig. 1a).<sup>24</sup> AC/MoO<sub>2</sub> was synthesized *via* grafting the (dme)MoO<sub>2</sub>Cl<sub>2</sub> precursor onto activated carbon, presumably *via* two proximate AC-OH  $\sigma$ -bonds, and was characterized by N<sub>2</sub>-TPD, H<sub>2</sub>-TPR, ICP-OES, and XPS, XANES, EXAFS and DFT.<sup>24</sup> This catalyst is air- and moisture-stable, highly recyclable, and exhibits remarkable catalytic flexibility in polyester plastic deconstruction and transesterification,<sup>24–26</sup> alcohol dehydration and alcohol dehydrogenation,<sup>27,28</sup> reductive carbonyl coupling and hydroboration,<sup>29,30</sup> and *N*-oxide reduction reactions.<sup>31</sup> To enhance understanding of AC/MoO<sub>2</sub> active site structure–activity–selectivity relationships, structurally better-defined graphene-based carbon supports, reduced graphene oxide (rGO),<sup>9</sup> carbon nanohorn (CNH),<sup>10</sup> and polyhydroxylated fullerenes<sup>32</sup> have been examined as promising supports. Furthermore, very pure carbon CNHs are particularly attractive, since they enable atomistic observation of catalytic sites using single-molecule atomic-resolution time-resolved electron microscopy (SMART-EM) without the risk of adventitious metal contamination.<sup>10</sup>

While the aforementioned studies surveyed the catalytic properties of carbon/metal–O<sub>2</sub> species over a wide range of carbons with metal fixed, the catalytic properties of both

homogenous and heterogeneous catalysts are known to vary widely and in useful ways between second and third-row metals in the same periodic table column.<sup>33–35</sup> For the present SSHC class, tungsten is attractive as a non-toxic cost-effective Mo analogue (Fig. 1b).<sup>36,37</sup> It has a lower environmental impact than Mo particularly in terms of carbon emissions and footprint during production.<sup>38</sup> Tungsten is highly stable in its 6+ oxidation state making it an effective catalyst to mediate redox reactions.<sup>39</sup> Furthermore, the higher atomic number of tungsten *versus* molybdenum offers higher contrast in transmission electron microscopy (TEM) to better trace catalytic events.<sup>40</sup>

Regarding representative W catalytic properties, tungsten alkylidenes are known to be excellent olefin metathesis catalysts<sup>41</sup> while tungsten sulfides are widely used hydrodesulfurization catalysts.<sup>42</sup> For both reactions, the respective W catalysts are industrially preferred over Mo due to their lower cost and superior activity, possibly reflecting W's greater polarizability and activation of certain substrate classes.<sup>43</sup> WO<sub>x</sub>-materials are also efficient catalysts and photocatalysts for various organic transformations, primarily coupling, oxidation processes, and heterocycle synthesis.<sup>44</sup> Metal oxide-supported WO<sub>3</sub> catalysts, such as TiO<sub>2</sub>–SiO<sub>2</sub>/WO<sub>3</sub>,<sup>45</sup> SnO<sub>2</sub>/WO<sub>3</sub>,<sup>46</sup> and Al<sub>2</sub>O<sub>3</sub>/WO<sub>3</sub>,<sup>47</sup> have proven activity in catalytic oxidations. Furthermore, reactivity studies of (WO<sub>3</sub>)<sub>3</sub> clusters supported on TiO<sub>2</sub> and FeO have demonstrated the importance of O=W=O species.<sup>48,49</sup>

Considering the established performance of carbon-supported SSHC MoO<sub>2</sub> catalysts, and the known activity of W=O moieties in other modes of catalysis, we investigate here the first third row carbon-supported tungsten-oxo SSHCs. This includes an effective synthesis, detailed characterization using ICP-OES, XPS, EXAFS, XANES, DFT, and SMART-EM, along with a compare/contrast activity/selectivity survey of AC/WO<sub>2</sub> *vs.* AC/MoO<sub>2</sub> catalysis. It will be seen that AC/WO<sub>2</sub> exhibits higher activity and selectivity in certain reactions and lower activity in others, for reasons that will be discussed.

## Results and discussion

### Synthesis of AC/WO<sub>2</sub> SSHC

Hexamethyldisiloxane was reacted with WOCl<sub>4</sub> in the presence of dry dimethoxyethane to yield white crystalline (DME)WO<sub>2</sub>Cl<sub>2</sub>,<sup>50</sup> with <sup>1</sup>H and <sup>13</sup>CNMR (500 MHz CD<sub>2</sub>Cl<sub>2</sub>) resonances at 4.15, 4.07 and 71.96, 65.72, respectively. Similar to the synthesis of AC/MoO<sub>2</sub>,<sup>24</sup> direct grafting of the (DME)WO<sub>2</sub>Cl<sub>2</sub> molecular precursor in CH<sub>2</sub>Cl<sub>2</sub> at 25 °C/18 h with

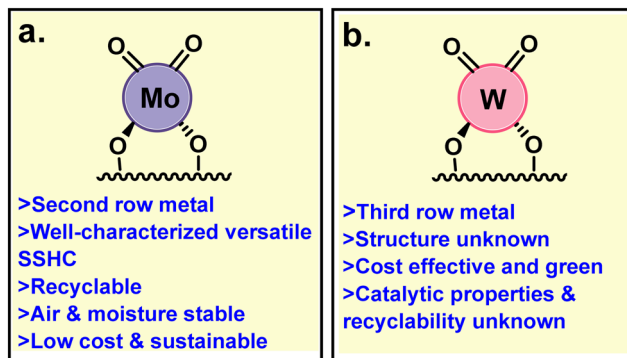
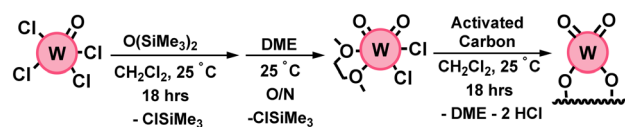


Fig. 1 (a) Structure and properties of activated carbon/MoO<sub>2</sub>, (b) unknown properties of the W analogue.



Scheme 1 Synthesis of single-site activated carbon-supported tungsten dioxo catalyst.



activated carbon yields the corresponding AC/WO<sub>2</sub> catalyst, HCl, and DME (Scheme 1).

### Characterization of AC/WO<sub>2</sub> SSHC

According to ICP-OES, AC/WO<sub>2</sub> has 2.80 wt% W loading which is comparable to previously reported AC/MoO<sub>2</sub> catalyst.<sup>24</sup> Due to the highly absorptive optical nature of activated carbon and low W loading, FTIR, Raman and UV-vis spectroscopy could not be employed to meaningfully characterize the catalytic sites. Thus, X-ray spectroscopic measurements were performed at the Advanced Photon Source (APS) at the Argonne National Laboratory (ANL) to understand the local electronic and geometric environment of the catalyst. W L<sub>III</sub>-edge energy at 10.208 keV against a tungsten foil at 10.205 keV was from X-Ray Absorption Near-Edge Spectroscopy (XANES) for AC/WO<sub>2</sub> (Fig. 2a). Comparing the XANES edge to various tungsten model compounds, WO<sub>2</sub>, WO<sub>3</sub>, and (DME)WO<sub>2</sub>Cl<sub>2</sub>, confirms the W oxidation state as +6 (Fig. 2a). XANES linear combination fitting was used to confirm the presence of only W(VI) species. The W 4f<sub>7/2</sub> X-Ray Photoelectron Spectroscopy (XPS) data show that AC/WO<sub>2</sub> has a feature at 35.9 eV, further confirming the presence of bound W(VI) species (Fig. 2b). Extended X-Ray Absorption Fine Structure Spectroscopy (EXAFS) fitting results reveal that

AC/WO<sub>2</sub> has two W=O bond distances of 1.68(2) Å and two W–O bond distances of 1.89(2) Å (Fig. 2c; Table 1), similar to the structures of previously reported AC/MoO<sub>2</sub>, rGO/MoO<sub>2</sub>, and CNH/MoO<sub>2</sub> catalysts, and WO<sub>2</sub>Cl<sub>2</sub>(dme).<sup>9,10,24</sup> These EXAFS-derived bond lengths agree with the DFT computational model (Fig. 2e). In addition, the precise bond lengths from the single-crystal X-ray diffraction measurement of a homogenous WO<sub>2</sub>Cl<sub>2</sub>(dme) model compound agree well with the supported catalysts.<sup>51</sup> We also provide the EXAFS fitting results for the (DME)WO<sub>2</sub>Cl<sub>2</sub> precursor and compare them to XRD to support the validity of XAS in studying SSHCs (Fig. 2d and Table 1).

Atomic-level identification of the reactive species on the catalyst surface of SSHCs, especially the connectivity between the support and the catalyst, presents a formidable challenge (Fig. 3). Our previous study on AC/MoO<sub>2</sub> catalysts found that ~50% of the supported Mo species are catalytically significant in transesterification processes.<sup>24</sup> These bulk-level data are supported by *in situ* SMART-EM analysis.<sup>10,52</sup> Thus, CHN/MoO<sub>2</sub> was found to contain both single and multi-metallic sites in a single/multi ratio of ~44:56.<sup>10</sup> In addition, upon using this catalyst for ethanol dehydrogenation, we identified only on the single sites the reaction intermediates predicted by DFT calculations along the reaction pathway, as well as polyacetal products verified by mass spectrometry.<sup>52</sup>

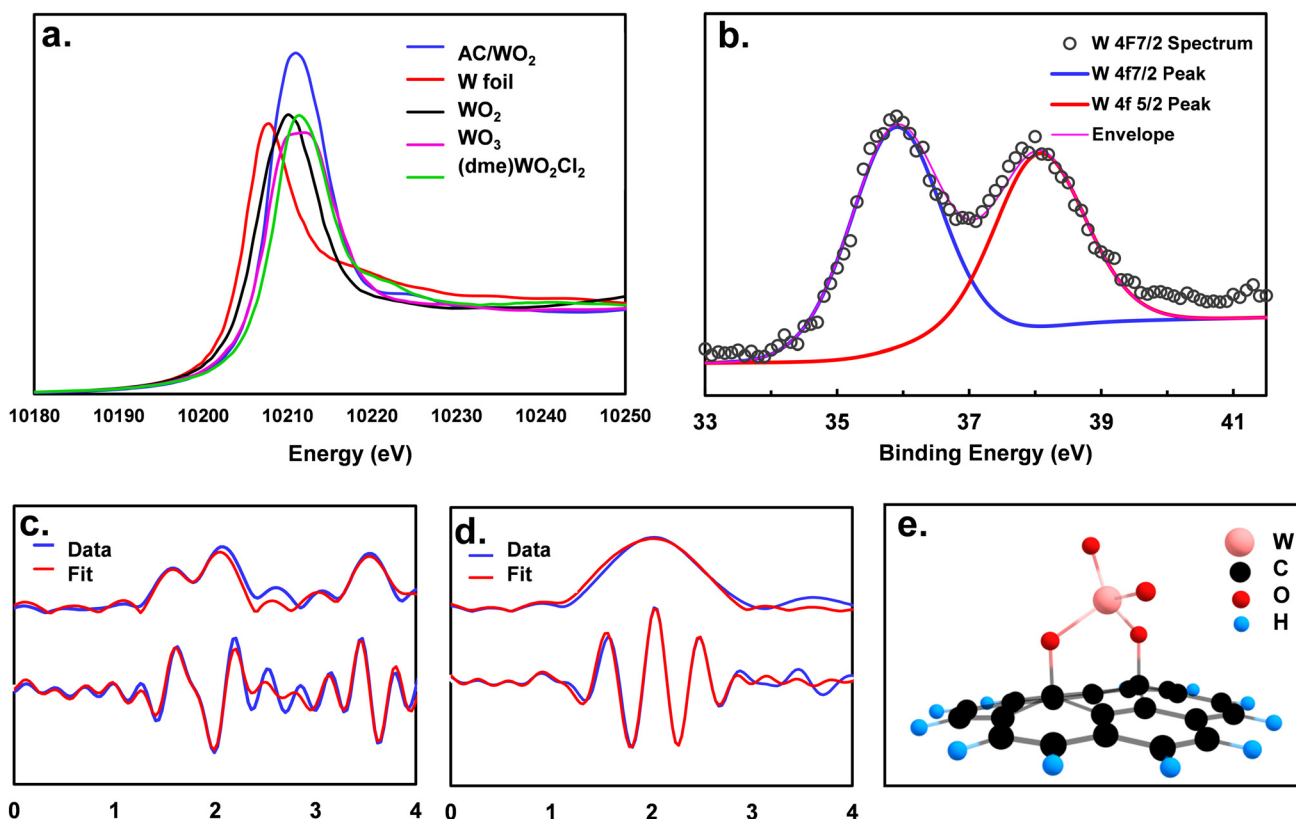


Fig. 2 Structural characterization of the AC/WO<sub>2</sub> catalyst: (a) XANES L<sub>III</sub>-edge energies for AC/WO<sub>2</sub> (blue), metal W (red), WO<sub>2</sub> (black), WO<sub>3</sub> (pink) and (dme)WO<sub>2</sub>Cl<sub>2</sub> (green) (b) W 4f XPS spectra for AC/WO<sub>2</sub> (c) EXAFS pRDFs magnitude (top) and real (bottom) for AC/WO<sub>2</sub> (d) EXAFS pRDFs magnitude (top) and real (bottom) for (dme)WO<sub>2</sub>Cl<sub>2</sub> and (e) DFT computed model for AC/WO<sub>2</sub>.



**Table 1** Data summary for AC/WO<sub>2</sub> structural characterization

Entry	Catalyst	Bond	XANES edge energy (keV)	EXAFS bond length (Å)	DFT bond length (Å)	EXAFS coordination
1	AC/WO <sub>2</sub>	W=O	10.208	1.73(2)	1.71	2
		W-O		1.92(2)	1.89	2
2	WO <sub>2</sub> Cl <sub>2</sub> (dme)	W=O	10.209	1.72(2)	1.708(3) <sup>a</sup>	2
		W-O		2.25(2)	2.272(3) <sup>a</sup>	2
		W-Cl		2.34(2)	2.356(3) <sup>a</sup>	2
		Mo=O		1.68(2)	1.68	2
3	AC/MoO <sub>2</sub> (ref. 9)	Mo=O	19.995	1.89(2)	1.87	2
		Mo-O				

<sup>a</sup> Average bond lengths from single-crystal XRD.

No such intermediates or products were detected on the multi-metallic sites by SMART-EM. In the present study, we likewise supported WO<sub>2</sub> on the same CNHs to determine the single/multi ratio (ESI† for details, Fig. S1–S4) and find a single-/multi-metal ratio of 44 : 56 – a ratio nearly identical to the above MoO<sub>2</sub> data.

In SMART-EM imaging, an atom is observed with a diameter approximately proportional to  $Z^{2/3}$ , where  $Z$  is the atomic number, and molecular structures can be illustrated with the Z-correlated (ZC) model like the one shown in Fig. 3d.<sup>53</sup> Tungsten ( $Z = 74$ ) is thus more readily observed as a larger dot than carbon ( $Z = 6$ ) or molybdenum ( $Z = 42$ ) which were reported in earlier studies.<sup>10,52</sup> Fig. 3a and b show representative TEM images of the WO<sub>2</sub> species on CNHs taken from videos at 20 millisecond per frame or 50 frames per second (fps). To enhance the image visibility, 20

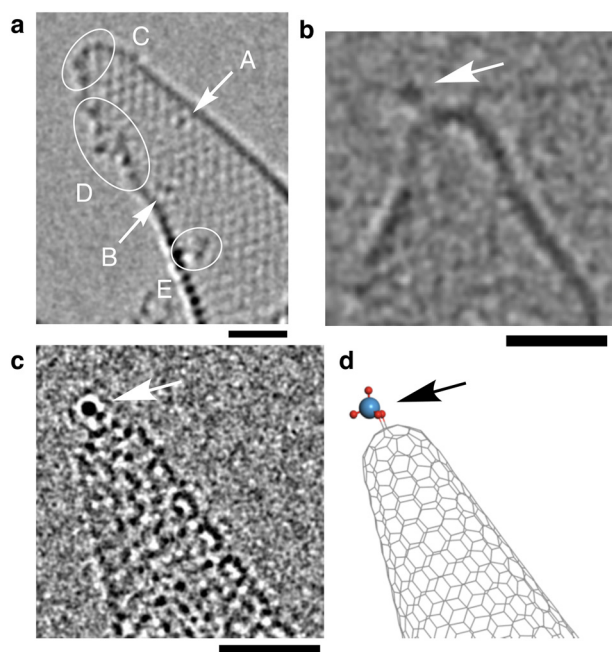
consecutive TEM images were superimposed in Fig. 3a (for original sequential images, see Fig. S1†). In regions A and B in Fig. 3a, we see single-site W species featuring out-of-plane bonding as depicted in Fig. 3b. TEM simulations based on the multi-slice method and the ZC model indicate the out-of-plane binding in the single metallic site (Fig. 3c and d).

Fig. 3 regions C–E show multi-metallic sites where the metal centers are bound roughly in large defective holes in the graphene plane.<sup>53</sup> Given the precedents for the MoO<sub>2</sub> catalysts discussed in the previous paragraph, we expect that the out-of-plane single metallic sites serve as reactive sites, while the sites with multiple WO<sub>2</sub> units are bound in-plane less unreactive (Fig. S4†). Indeed bound catalytic intermediates are only observed SMART-EM for the monometallic sites.<sup>52</sup>

### Catalytic properties of AC/WO<sub>2</sub> vs. AC/MoO<sub>2</sub>

Lastly, in this study, we were interested in comparing the activity of the new AC/WO<sub>2</sub> catalyst against the well-studied AC/MoO<sub>2</sub> analog to study the metal effects of this supported system. Here, we report the activity of these catalysts for three classical benchmark reactions for such systems, namely, dehydration of alcohols to alkenes (Scheme 2a–g), epoxidation of alkenes to oxiranes (Scheme 2h), and deconstruction of polyethylene terephthalate (PET) (Scheme 2i). All these reactions have been previously reported for the AC/MoO<sub>2</sub> catalytic system for a wide variety of substrates, kinetic measurements, and detailed mechanistic analyses.<sup>28</sup>

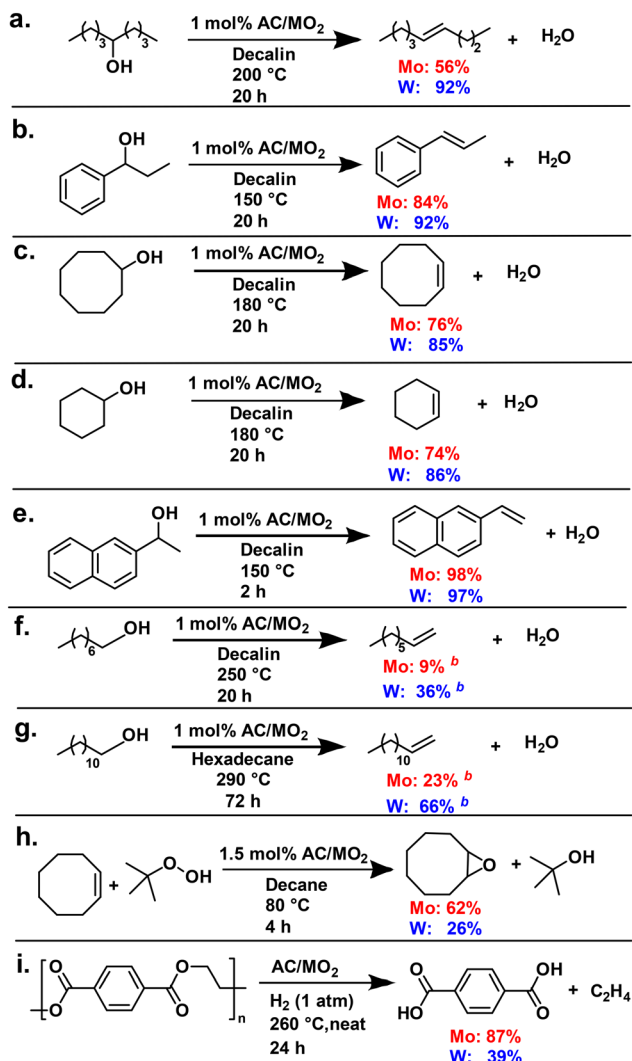
For dehydration of 5-nonanol to 5-nonene at 1 mol% catalyst and 200 °C for 20 hours, a high yield of 92% for AC/WO<sub>2</sub> and a moderate yield of 56% for AC/MoO<sub>2</sub> is achieved (Scheme 2a). A similar trend is observed for the dehydration of aromatic and cyclic secondary alcohols. For 1-phenyl-1-propanol to 1-phenyl-1-propene dehydration, a 92% yield with AC/WO<sub>2</sub> and an 84% yield with AC/MoO<sub>2</sub> is achieved (Scheme 2b). For cyclooctanol to cyclooctene dehydration, an 85% yield with AC/WO<sub>2</sub> and a 76% yield with AC/MoO<sub>2</sub> are obtained (Scheme 2c). For cyclohexanol to cyclohexene dehydration, an 86% yield with AC/WO<sub>2</sub> and a 74% yield with AC/MoO<sub>2</sub> are obtained (Scheme 2d). Naphthyl ethanol affords full conversion within 2 h at 150 °C selectively yielding vinyl naphthalene for both the catalysts (Scheme 2e).



**Fig. 3** Representative SMART-EM images of CNH/WO<sub>2</sub>; scale bars: 1 nm. (a) Experimental TEM image after 20 stacks. White arrows and circle indicate single (A and B) and multiple sites (C–E), respectively (Fig. S2†). (b) Out-of-plane WO<sub>2</sub> on CNH. (c and d) TEM simulation and ZC model for out-of-plane model. EDR (electron dose rate) =  $5.7\text{--}7.2 \times 10^6 \text{ e}^- \text{ nm}^{-2} \text{ s}^{-1}$ .







**Scheme 2** Activity of AC/WO<sub>2</sub> compared to AC/MoO<sub>2</sub> for (a)–(g) alcohol dehydration (h) alkene epoxidation, and (i) PET deconstruction.<sup>a</sup> Yields quantified using <sup>1</sup>H NMR with mesitylene as internal standard. <sup>b</sup>Mixture of isomers.

Next, the dehydration of primary alcohols was investigated which was previously found for the AC/MoO<sub>2</sub> system to present activity and selectivity challenges.<sup>28</sup> The selective dehydration of primary aliphatic alcohols is particularly relevant to biomass conversion and organic synthesis.<sup>54,55</sup> For the dehydration of 1-octanol, a 36% yield of the dehydration product (octene) was observed for AC/WO<sub>2</sub> compared to 9% for AC/MoO<sub>2</sub> (Scheme 2f). Note that a mixture of octene isomers is found in both cases, as has been previously reported for the dehydration of primary alcohols in other catalytic systems.<sup>56</sup> Numerous studies have linked the higher dehydration activity of tungsten oxides to the higher Lewis acidity of W compared to Mo.<sup>57–59</sup> Furthermore, no dehydrogenation product (octanal) was formed with AC/WO<sub>2</sub> which was the major product for AC/MoO<sub>2</sub> (12%). This difference for W vs. Mo where for the former, the dehydration channel is preferred and for the latter, dehydrogenation is

preferred for primary alcohols has been reported for (WO<sub>3</sub>)<sub>3</sub>, and (MoO<sub>3</sub>)<sub>3</sub> clusters.<sup>57</sup> Overall less side products such as condensation products (ethers) are observed with a higher selectivity for dehydration with AC/WO<sub>2</sub> versus AC/MoO<sub>2</sub> (53% vs. 12% selectivity for octene). Under harsher conditions (290 °C, 72 hours), a respectable yield of 66% is obtained for the dehydration of 1-dodecanol to dodecene for the W catalyst compared to a 23% yield for the Mo catalyst (Scheme 2g). Overall, AC/WO<sub>2</sub> is a superior catalyst for alcohol dehydration compared to AC/MoO<sub>2</sub>. To demonstrate the recyclability of AC/WO<sub>2</sub>, the catalyst was filtered, washed and dried and reused for 5-nonanol dehydration (Scheme 2a). There was no change in activity upon recycling the catalyst once, yielding 90% of 5-nonene after 20 hours at 200 °C, demonstrating its practical utility. From ICP-OES analysis, no change in W wt% was observed suggesting negligible leaching.

For the epoxidation of cyclooctene to cyclooctene-oxide, AC/MoO<sub>2</sub> is more active than AC/WO<sub>2</sub> under identical conditions of 1.5 mol% catalyst at 80 °C for 4 hours (62 vs. 26% yield) (Scheme 2h). This observation is consistent with existing literature on WO<sub>x</sub>- and MoO<sub>x</sub>-mediated alkene epoxidation.<sup>60,61</sup> Next, for polyethylene terephthalate (PET) hydrogenolysis, AC/MoO<sub>2</sub> is more active than AC/WO<sub>2</sub> under identical conditions (87 vs. 39% yield) (Scheme 2i). Overall, these reactivity differences can be attributed to the differences in electronic structure and related acid–base properties of Mo and W oxo complexes. These intriguing results should inform further research on carbon-supported metal-oxo SSHCs to broaden the reaction scope and mechanistic understanding of such catalytic materials.

## Conclusions

We report the synthesis of a new activated carbon-supported dioxo-tungsten SSHC. Detailed characterization of this catalyst was performed using ICP-OES, XPS, XANES, EXAFS, and SMART-EM. The presence of the 6+ tungsten species was confirmed using XPS and XANES. The W EXAFS data fitting identifies two W=O double bond lengths at 1.7 Å and two W–O single bond lengths at 1.9 Å. These data closely align with DFT computational results, reinforcing the proposed catalyst structure as AC(–μ-O–)<sub>2</sub>M(=O)<sub>2</sub>, analogous to the previously reported AC/MoO<sub>2</sub> catalyst. In addition, single W sites are identified by SMART-EM as having out-of-plane bonds on the CNH surface, consistent with the structure of a catalytic species. Statistical analysis based on direct observation of single and multiple sites confirms the structure–catalytic activity relationship and provides direct information on the structural aspects of the SSHC. Finally, the novel tungsten catalyst is more active and selective than the molybdenum catalyst in mediating alcohol dehydration of various substrates. Most notably, AC/WO<sub>2</sub> is an effective and recyclable catalyst for dehydration of primary aliphatic alcohols and forms no dehydrogenation side products unlike



AC/MoO<sub>2</sub>. Both these catalysts are highly stable and recyclable for this transformation. Lastly, for epoxidation of cyclooctene and hydrogenolysis of PET, AC/MoO<sub>2</sub> continues to be the superior catalyst compared to AC/WO<sub>2</sub>. The synthesis, characterization and preliminary activity of this novel catalytic system should motivate further research in carbon-supported SSHCs specifically aimed at understanding and productively utilizing metal effects in these systems including understanding stability trends.

## Data availability

The data supporting this article have been included as part of the ESI.†

## Conflicts of interest

There are no conflicts to declare.

## Acknowledgements

Financial support was provided by the U.S. Department of Energy, Office of Science, Office of Basic Energy by Award Number DOE DE-SC0024448 at Northwestern University (NU). This work made use of IMSERC facilities at NU, which have received support from Soft and Hybrid Nanotechnology Experimental (SHyNE) Resource (NSF ECCS-2025633), Int. Institute of Nanotechnology, and NU. This work made use of NU QBIC generously supported by NASA Ames Research Center Grant NNA04CC36G. This work used the DuPont-Northwestern-Dow Collaborative Access Team (DND-CAT) 5BM-D beamline at the Advanced Photon Source (APS). DND-CAT is supported by NU, E. I. DuPont de Nemours & Co., and The Dow Chemical Company. The APS is supported by DOE at Argonne National Laboratory under Contract DE-AC02-06CH11357. Additionally, this work made use of the REACT Facility of NU's Center for Catalysis and Surface Science supported by a grant from the DOE (DE-SC0001329). This research was supported in part by the computational resources and staff contributions provided by the Quest High Performance Computing Facility at NU, which is jointly supported by the Office of the Provost, the Office for Research, and NU Information Technology. This research was also supported by JSPS KAKENHI (JP23H04874, and 24H00447). This research was also supported by the PRESTO program from JST (JPMJPR23Q6). MH thanks the Fellowship (JSPS and MERIT-WINGS).

## References

- 1 A. Wang, J. Li and T. Zhang, Heterogeneous single-atom catalysis, *Nat. Rev. Chem.*, 2018, **2**(6), 65–81.
- 2 D. Cole-Hamilton and R. Tooze, Homogeneous catalysis—advantages and problems, *Catalyst Separation, Recovery and Recycling: Chemistry and Process Design*, 2006, pp. 1–8.
- 3 C. Copéret, F. Allouche, K. W. Chan, M. P. Conley, M. F. Delley and A. Fedorov, *et al.*, Bridging the Gap between Industrial and Well-Defined Supported Catalysts, *Angew. Chem., Int. Ed.*, 2018, **57**(22), 6398–6440.
- 4 C. Copéret, A. Comas-Vives, M. P. Conley, D. P. Estes, A. Fedorov and V. Mougel, *et al.*, Surface organometallic and coordination chemistry toward single-site heterogeneous catalysts: strategies, methods, structures, and activities, *Chem. Rev.*, 2016, **116**(2), 323–421.
- 5 M. S. Eisen and T. J. Marks, Supported organoactinide complexes as heterogeneous catalysts. A kinetic and mechanistic study of facile arene hydrogenation, *J. Am. Chem. Soc.*, 1992, **114**(26), 10358–10368.
- 6 M. M. Stalzer, M. Delferro and T. J. Marks, Supported single-site organometallic catalysts for the synthesis of high-performance polyolefins, *Catal. Lett.*, 2015, **145**, 3–14.
- 7 J. M. Thomas, R. Raja and D. W. Lewis, Single-site heterogeneous catalysts, *Angew. Chem., Int. Ed.*, 2005, **44**(40), 6456–6482.
- 8 S. L. Wegener, T. J. Marks and P. C. Stair, Design Strategies for the Molecular Level Synthesis of Supported Catalysts, *Acc. Chem. Res.*, 2012, **45**(2), 206–214.
- 9 Y. Liu, J. Li, A. Das, H. Kim, L. O. Jones and Q. Ma, *et al.*, Synthesis and Structure–Activity Characterization of a Single-Site MoO<sub>2</sub> Catalytic Center Anchored on Reduced Graphene Oxide, *J. Am. Chem. Soc.*, 2021, **143**(51), 21532–21540.
- 10 Y. Kratish, T. Nakamuro, Y. Liu, J. Li, I. Tomotsuka and K. Harano, *et al.*, Synthesis and Characterization of a Well-Defined Carbon Nanohorn-Supported Molybdenum Dioxo Catalyst by SMART-EM Imaging. Surface Structure at the Atomic Level, *Bull. Chem. Soc. Jpn.*, 2020, **94**(2), 427–432.
- 11 Z. Zhuang, J. Huang, Y. Li, L. Zhou and L. Mai, The holy grail in platinum-free electrocatalytic hydrogen evolution: molybdenum-based catalysts and recent advances, *ChemElectroChem*, 2019, **6**(14), 3570–3589.
- 12 Y. Zhou, W. Wang, C. Zhang, D. Huang, C. Lai and M. Cheng, *et al.*, Sustainable hydrogen production by molybdenum carbide-based efficient photocatalysts: From properties to mechanism, *Adv. Colloid Interface Sci.*, 2020, **279**, 102144.
- 13 G. Schwarz, R. R. Mendel and M. W. Ribbe, Molybdenum cofactors, enzymes and pathways, *Nature*, 2009, **460**(7257), 839–847.
- 14 J. Mol, Industrial applications of olefin metathesis, *J. Mol. Catal. A: Chem.*, 2004, **213**(1), 39–45.
- 15 D. L. Lourenço and A. C. Fernandes, HBpin/MoO<sub>2</sub>Cl<sub>2</sub> (H<sub>2</sub>O)<sub>2</sub> as an efficient catalytic system for the reduction of esters, lactones and polyester plastic waste, *Mol. Catal.*, 2023, **542**, 113128.
- 16 R. Hernandez-Ruiz and R. Sanz, Dichlorodioxomolybdenum (VI) complexes: useful and readily available catalysts in organic synthesis, *Synthesis*, 2018, **50**(20), 4019–4036.
- 17 F. Zhai, K. V. Bukhryakov, R. R. Schrock, A. H. Hoveyda, C. Tsay and P. Müller, Syntheses of molybdenum oxo benzylidene complexes, *J. Am. Chem. Soc.*, 2018, **140**(42), 13609–13613.
- 18 K. V. Bukhryakov, R. R. Schrock, A. H. Hoveyda, C. Tsay and P. Müller, Syntheses of molybdenum oxo alkylidene



- complexes through addition of water to an alkylidyne complex, *J. Am. Chem. Soc.*, 2018, **140**(8), 2797–2800.
- 19 H. I. Karunadasa, C. J. Chang and J. R. Long, A molecular molybdenum-oxo catalyst for generating hydrogen from water, *Nature*, 2010, **464**(7293), 1329–1333.
  - 20 K. Jeyakumar and D. K. Chand, Application of molybdenum (VI) dichloride dioxide ( $\text{MoO}_2\text{Cl}_2$ ) in organic transformations, *J. Chem. Sci.*, 2009, **121**(2), 111–123.
  - 21 N. Garcia, M. A. Fernández-Rodríguez, P. García-García, M. R. Pedrosa, F. J. Arnaiz and R. Sanz, A practical and chemoselective Mo-catalysed sulfoxide reduction protocol using a 3-mercaptopropyl-functionalized silica gel (MPS), *RSC Adv.*, 2016, **6**(32), 27083–27086.
  - 22 H. Arzoumanian, Molybdenum-oxo chemistry in various aspects of oxygen atom transfer processes, *Coord. Chem. Rev.*, 1998, **178**, 191–202.
  - 23 S. C. Sousa, I. Cabrita and A. C. Fernandes, High-valent oxomolybdenum and oxo-rhenium complexes as efficient catalysts for X–H (X= Si, B, P and H) bond activation and for organic reductions, *Chem. Soc. Rev.*, 2012, **41**(17), 5641–5653.
  - 24 A. R. Mouat, T. L. Lohr, E. C. Wegener, J. T. Miller, M. Delferro and P. C. Stair, *et al.*, Reactivity of a Carbon-Supported Single-Site Molybdenum Dioxo Catalyst for Biodiesel Synthesis, *ACS Catal.*, 2016, **6**(10), 6762–6769.
  - 25 Y. Kratish, J. Li, S. Liu, Y. Gao and T. J. Marks, Polyethylene Terephthalate Deconstruction Catalyzed by a Carbon-Supported Single-Site Molybdenum-Dioxo Complex, *Angew. Chem., Int. Ed.*, 2020, **59**(45), 19857–19861.
  - 26 Y. Liu, A. Agarwal, Y. Kratish and T. J. Marks, Single-Site Carbon-Supported Metal-Oxo Complexes in Heterogeneous Catalysis: Structure, Reactivity, and Mechanism, *Angew. Chem., Int. Ed.*, 2023, e202304221.
  - 27 T. L. Lohr, A. R. Mouat, N. M. Schweitzer, P. C. Stair, M. Delferro and T. J. Marks, Efficient catalytic greenhouse gas-free hydrogen and aldehyde formation from aqueous alcohol solutions, *Energy Environ. Sci.*, 2017, **10**(7), 1558–1562.
  - 28 J. Li, A. Das, Q. Ma, M. J. Bedzyk, Y. Kratish and T. J. Marks, Diverse Mechanistic Pathways in Single-Site Heterogeneous Catalysis: Alcohol Conversions Mediated by a High-Valent Carbon-Supported Molybdenum-Dioxo Catalyst, *ACS Catal.*, 2022, **12**(2), 1247–1257.
  - 29 S. Liu, J. Li, T. Jurca, P. C. Stair, T. L. Lohr and T. J. Marks, Efficient carbon-supported heterogeneous molybdenum-dioxo catalyst for chemoselective reductive carbonyl coupling, *Catal. Sci. Technol.*, 2017, **7**(11), 2165–2169.
  - 30 Y. Liu, A. Agarwal, L. Ye, Y. Kratish and T. J. Marks, Aldehyde and Ketone Hydroboration Mediated by a Heterogeneous Single-Site Molybdenum-Dioxo Catalyst: Scope and Mechanistic Implications, *ChemCatChem*, 2024, **16**(7), e202301417.
  - 31 J. Li, S. Liu, T. L. Lohr and T. J. Marks, Efficient Chemoselective Reduction of N-Oxides and Sulfoxides Using a Carbon-Supported Molybdenum-Dioxo Catalyst and Alcohol, *ChemCatChem*, 2019, **11**(16), 4139–4146.
  - 32 A. Agarwal, Y. Liu, O. A. Kraevaya, S. Alayoglu, Y. Kratish and T. J. Marks, Models for Single-Site Heterogeneous Catalysts on Carbon: MoO<sub>2</sub> Epoxidation Catalyst Anchored to a Fullerene, *ChemCatChem*, 2024, e202401259.
  - 33 J. R. Ludwig and C. S. Schindler, Catalyst: sustainable catalysis, *Chem*, 2017, **2**(3), 313–316.
  - 34 M. P. Watson and D. J. Weix, The Once and Future Catalysts: How the Challenges of First-Row Transition-Metal Catalysis Grew to Become Strengths, *Acc. Chem. Res.*, 2024, 2451–2452.
  - 35 A. Haynes, Carbonylations Promoted by Third-Row Transition Metal Catalysts, *Carbon Monoxide in Organic Synthesis: Carbonylation Chemistry*, 2021, pp. 333–362.
  - 36 Tungsten Oxide Price, CNY/mt SMM [available from: <https://www.metal.com/Tungsten/202209270001?form=MG0AV3>].
  - 37 High-purity Molybdenum Trioxide Price, CNY/mt SMM [available from: <https://www.metal.com/Other-Minor-Metals/202201210001?form=MG0AV3>].
  - 38 N. V. Reutova, T. V. Reutova, F. R. Dreeva and A. A. Shevchenko, Long-term impact of the Tyrnyauz tungsten-molybdenum mining and processing factory waste on environmental pollution and children's population, *Environ. Geochem. Health*, 2022, **44**(12), 4557–4568.
  - 39 Z. F. Huang, J. Song, L. Pan, X. Zhang, L. Wang and J. J. Zou, Tungsten oxides for photocatalysis, electrochemistry, and phototherapy, *Adv. Mater.*, 2015, **27**(36), 5309–5327.
  - 40 J. Xing, K. Takeuchi, K. Kamei, T. Nakamuro, K. Harano and E. Nakamura, Atomic-number (Z)-correlated atomic sizes for deciphering electron microscopic molecular images, *Proc. Natl. Acad. Sci. U. S. A.*, 2022, **119**(14), e2114432119.
  - 41 N. Barteczko, M. Grymel and A. Chrobok, Heterogeneous catalysts for olefin metathesis, *Catal. Commun.*, 2023, **177**, 106662.
  - 42 P. Vasudevan and J. G. Fierro, A review of deep hydrodesulfurization catalysis, *Catal. Rev.:Sci. Eng.*, 1996, **38**(2), 161–188.
  - 43 G. D. Rieck, *Tungsten and its Compounds*, Elsevier, 2013.
  - 44 K. Aravindraj and S. Mohana Roopan, WO<sub>3</sub>-based materials as heterogeneous catalysts for diverse organic transformations: a mini-review, *Synth. Commun.*, 2022, **52**(13–14), 1457–1476.
  - 45 R. Jin, X. Xia, W. Dai, J. F. Deng and H. Li, An effective heterogeneous WO<sub>3</sub>/TiO<sub>2</sub>-SiO<sub>2</sub> catalyst for selective oxidation of cyclopentene to glutaraldehyde by H<sub>2</sub>O<sub>2</sub>, *Catal. Lett.*, 1999, **62**(2), 201–207.
  - 46 Z. Zhang, Q. Zhu, J. Ding, X. Liu and W.-L. Dai, Effect of calcination temperature of the support and the catalyst of WO<sub>3</sub>/SnO<sub>2</sub> on the catalytic oxidation of 1,2-benzenedimethanol by H<sub>2</sub>O<sub>2</sub>, *Appl. Catal., A*, 2014, **482**, 171–178.
  - 47 Y. Zhu, J. Xu and M. Lu, Oxidation of primary and secondary alcohols to the corresponding carbonyl compounds with molecular oxygen using 1,1-diphenyl-2-picrylhydrazyl and WO<sub>3</sub>/Al<sub>2</sub>O<sub>3</sub> as catalysts, *Catal. Commun.*, 2014, **48**, 78–84.
  - 48 Y. K. Kim, R. Rousseau, B. D. Kay, J. M. White and Z. Dohnálek, Catalytic Dehydration of 2-Propanol on (WO<sub>3</sub>)<sub>3</sub> Clusters on TiO<sub>2</sub>(110), *J. Am. Chem. Soc.*, 2008, **130**(15), 5059–5061.



- 49 S.-C. Li, Z. Li, Z. Zhang, B. D. Kay, R. Rousseau and Z. Dohnálek, Preparation, Characterization, and Catalytic Properties of Tungsten Trioxide Cyclic Trimers on FeO(111)/Pt(111), *J. Phys. Chem. C*, 2012, **116**(1), 908–916.
- 50 K. Dreisch, C. Andersson and C. St, Synthesis and structure of dimethoxyethane-dichlorodioxo-tungsten (VI)—a highly soluble derivative of tungsten dioxodichloride, *Polyhedron*, 1991, **10**(20–21), 2417–2421.
- 51 M. F. Davis, W. Levason, M. E. Light, R. Ratnani, G. Reid and K. Saraswat, Tungsten (VI) and Molybdenum (VI) Complexes with Soft Thioether Ligand Coordination–Synthesis, Spectroscopic and Structural Studies, *Eur. J. Inorg. Chem.*, 2007, **13**, 1903–1910.
- 52 Y. Kratish, Y. Liu, J. Li, A. Das, L. O. Jones and A. Agarwal, *et al.*, Atomic-Resolution Cinematography of Catalytic Intermediates over a Single-Site Heterogeneous Catalyst, *ChemRxiv*, 2024, preprint, DOI: [10.26434/chemrxiv-2024-hpbl9](https://doi.org/10.26434/chemrxiv-2024-hpbl9).
- 53 A. Hashimoto, H. Yorimitsu, K. Ajima, K. Suenaga, H. Isobe and J. Miyawaki, *et al.*, Selective deposition of a gadolinium (III) cluster in a hole opening of single-wall carbon nanohorn, *Proc. Natl. Acad. Sci. U. S. A.*, 2004, **101**(23), 8527–8530.
- 54 Y. Kikuchi, M. Hirao, K. Narita, E. Sugiyama, S. Oliveira and S. Chapman, *et al.*, Environmental performance of biomass-derived chemical production: a case study on sugarcane-derived polyethylene, *J. Chem. Eng. Jpn.*, 2013, **46**(4), 319–325.
- 55 D. J. Ward, D. J. Saccomando, G. Walker and S. M. Mansell, Sustainable routes to alkenes: applications of homogeneous catalysis to the dehydration of alcohols to alkenes, *Catal. Sci. Technol.*, 2023, **13**(9), 2638–2647.
- 56 B. H. Davis and W. S. Brey Jr., Dehydration and dehydrogenation of 2-octanol by thorium oxide, *J. Catal.*, 1972, **25**(1), 81–92.
- 57 R. Rousseau, D. A. Dixon, B. D. Kay and Z. Dohnálek, Dehydration, dehydrogenation, and condensation of alcohols on supported oxide catalysts based on cyclic (WO<sub>3</sub>)<sub>3</sub> and (MoO<sub>3</sub>)<sub>3</sub> clusters, *Chem. Soc. Rev.*, 2014, **43**(22), 7664–7680.
- 58 Z. Li, Z. Fang, M. S. Kelley, B. D. Kay, R. Rousseau and Z. Dohnálek, *et al.*, Ethanol conversion on cyclic (MO<sub>3</sub>)<sub>3</sub> (M= Mo, W) clusters, *J. Phys. Chem. C*, 2014, **118**(9), 4869–4877.
- 59 M. Badlani and I. E. Wachs, Methanol: a “smart” chemical probe molecule, *Catal. Lett.*, 2001, **75**, 137–149.
- 60 K. A. Jørgensen, Transition-metal-catalyzed epoxidations, *Chem. Rev.*, 1989, **89**(3), 431–458.
- 61 P. Sözen-Aktaş, E. Manoury, F. Demirhan and R. Poli, Molybdenum versus tungsten for the epoxidation of cyclooctene catalyzed by [Cp\*<sub>2</sub>MoO<sub>5</sub>], *Eur. J. Inorg. Chem.*, 2013, **2013**(15), 2728–2735.

